A dielectric response study of the electronic stopping power of liquid water for energetic protons and a new *I*-value for water

D Emfietzoglou[1], R Garcia-Molina[2], I Kyriakou[1], I Abril[3] and H Nikjoo[4,5]

[1] Medical Physics Laboratory, University of Ioannina Medical School, Ioannina 451 10, Greece
[2] Departamento de Física - CIOyN, Universidad de Murcia, Apartado 4021, E-30080 Murcia, Spain
[3] Departament de Física Aplicada, Universitat d'Alacant, Apartat 99, E-03080 Alacant, Spain
[4] Department of Medical Radiation Physics, Karolinska Institute, Box 260, SE-171 76 Stockholm, Sweden

E-mail: Hooshang.nikjoo@ki.se

Abstract

The electronic stopping power of liquid water for protons over the 50 keV to 10 MeV energy range is studied using an improved dielectric response model which is in good agreement with the best available experimental data. The mean excitation energy (*I*) of stopping power theory is calculated to be 77.8 eV. Shell corrections are accounted for in a self-consistent manner through analytic dispersion relations for the momentum dependence of the dielectric function. It is shown that widely used dispersion schemes based on the random-phase approximation (RPA) can result in sizeable errors due to the neglect of damping and local field effects that lead to a momentum broadening and shifting of the energy-loss function. Low-energy Born corrections for the Barkas, Bloch and charge-state effects practically cancel out down to 100 keV proton energies. Differences with ICRU Report 49 stopping power values and earlier calculations are found to be at the ~20% level in the region of the stopping maximum. The present work overcomes the limitations of the Bethe formula below 1 MeV and improves the accuracy of previous calculations through a more consistent account of the dielectric response properties of liquid water.

(Some figures in this article are in colour only in the electronic version)

1. Introduction

The stopping power (also called stopping force) of liquid water for protons is a quantity of fundamental importance to hadron therapy and biophysics (Nikjoo *et al* 2008). Presently,

---

[5] Author to whom any correspondence should be addressed.

there are over 25 ion therapy facilities worldwide most of which use proton beams either exclusively or in addition to other light ions (Sisterson 2005). The advantage of using ion beams for cancer therapy is well understood and is principally due to their favorable absorbed dose distribution in matter with the characteristic Bragg peak profile (Brahme 2004). This, in combination with the limited lateral diffusion, allows substantially higher doses to deep-seated tumors and a sparing effect to shallow normal tissue compared to the conventional electron or photon beams (Smith 2006).

At high but non-relativistic energies, the electronic stopping due to ionization and excitation of target electrons represents the dominant energy-loss process. Among several available theories (Sigmund 2004), the Bethe theory (Inokuti 1971, 1996, Inokuti *et al* 1978) represents a standard framework for obtaining reasonably accurate values for light ions over a wide range of materials (Bichsel 1988, Sigmund 1998, Ziegler 1999, Sabin and Oddershede 2005). The only non-trivial parameter is the mean excitation energy of the material, the so-called *I*-value, which represents the main source of uncertainty in Bethe's formula at high energies (Inokuti 1971, 1996, Inokuti *et al* 1978). The *I*-value for condensed materials is often determined through either stopping power (and range) measurements or optical absorption data (ICRU 1984, 1993, 2005). Both methods, however, have their problems. For example, stopping measurements are usually carried out at ion energies where the various low-energy corrections to Bethe's formula are sizeable and, therefore, any experimental uncertainties are further augmented by the uncertainties of the correction terms used in the analysis (Kamakura *et al* 2006). On the other hand, optical data should practically cover a sufficiently large part of the absorption spectrum to exhaust the K-shell contribution (typically up to 10–100 keV); such a complete and consistent set of data is often hard to find (Smith *et al* 2006). The *I*-value of liquid water in the context of ion dosimetry has been discussed in a series of recent papers by Paul (Paul 2007a, 2007b, Paul *et al* 2007a, 2007b).

Going from higher to lower proton energies, the penetration ability of protons diminishes and, when below $\sim$1 MeV, their residual range in tissue becomes less than the resolution of the treatment planning algorithm used ($\sim$0.1–1 mm). Such low-energy protons are of particular importance from a biophysical perspective because it is the energy regime where the Bragg peak develops ($\sim$0.1 MeV) and, as a result, the particles exhibit their highest RBE (Paganetti *et al* 2002). Recently, two Monte Carlo codes for simulating full-slowing-down proton tracks in different phases of water have been developed (Uehara *et al* 2001, Friedland *et al* 2003) and the physics of slow proton stopping has been discussed (Uehara *et al* 2000, Dingfelder *et al* 2000). A fundamental problem in extending Bethe's formula down to the Bragg peak region is that its two main assumptions, namely the Born and dipole approximations, become gradually invalid (Sigmund 1994). Specifically, as the projectile velocity decreases, the minimum momentum transfer increases and non-dipole collisions become important rendering the dipole approximation invalid. The effect is more pronounced for inner shells associated with large binding energies, the contribution of which to the stopping process gradually vanishes (Basbas 1984). The so-called shell corrections to Bethe's formula are meant to account for the above effect (ICRU 1993). Unfortunately, the formal evaluation of shell corrections proceeds through the, generally unknown, generalized oscillator strength (GOS) or, for condensed targets, the momentum-dependent dielectric response function (Fano 1963). A standard approach is to employ hydrogen-like GOSs for the inner shells and scaling laws for the outer shells ignoring any aggregation and phase effects (ICRU 1993). Recent progress along this line has been reported by Bichsel (2002).

An alternative approach suitable for the condensed phase is to use a model dielectric response function analytic over the whole energy–momentum plane (Ritchie 1982). Apart from the evaluation of shell corrections, this method allows for the direct calculation of the

electronic stopping power in the Born approximation without resorting to Bethe's dipole approximation. The Lindhard electron gas dielectric function based on the random phase approximation (RPA) has offered a practical tool to an otherwise complicated theoretical problem (Echenique *et al* 1990, Pitarke and Campillo 2000). Non-RPA effects associated with damping (Mermin 1970) and local field corrections (Dabrowski 1986) have also been included in ion stopping calculations for condensed matter (Ashley 1980, Wang and Ma 1990, Schinner *et al* 1994). Recent advances along these lines are reported, for example, by Montanari and Miraglia (2006) and Barriga-Carrasco (2008).

Since an analytic dielectric function from first principles (similar to Lindhard's) is not available for realistic materials, Ritchie and Howie (1977) suggested a semi-empirical scheme whereby experimental optical data are used to give the dependence on energy loss while physically motivated 'extension' schemes provide the dependence on momentum transfer. Besides its simplicity, the main advantage of the Ritchie–Howie approach is that the use of optical data specific to the material under consideration automatically accounts for electronic structure effects in a realistic manner not always possible within the 'electron gas' models.

Ashley (1991) first applied the Ritchie–Howie recipe to proton stopping in solids using a very simple extension scheme based on the (undamped) plasmon-pole approximation with a quadratic dispersion. A more sophisticated approach using the Mermin dielectric function has been later advanced by Garcia-Molina and co-workers and applied to a variety of solid targets (e.g. Abril *et al* 1998, Denton *et al* 2008). Ion stopping calculations for liquid water and other condensed biomaterials along the Ritchie–Howie scheme have been recently undertaken by Dingfelder *et al* (2000), Akkerman *et al* (2001), Tan *et al* (2006, 2008), Emfietzoglou *et al* (2006a, 2006b, 2007a) and Garcia-Molina *et al* (2009). Calculations mainly differ on the extension scheme used since experimental data for condensed targets at finite momentum transfer are scarce. Several extension schemes of RPA origin have been proposed and, for liquid water, critically evaluated by Emfietzoglou *et al* (2006c, 2007b, 2008) who clearly demonstrated the importance of including non-RPA dispersion effects.

Finally, at energies near the stopping maximum, corrections to the Born approximation must be included. These generally account for higher order perturbation terms and for the changing charge state of the projectile (Brandt 1982, Basbas 1984, Sigmund 1994). Although these corrections are generally small above 50–100 keV u^{-1}, they will be considered here for completeness. Energy losses due to charge-transfer processes, which dominate the stopping power at even lower energies, are not considered here.

In the present work, we report calculations of the electronic stopping power of liquid water for protons over the 50 keV to 10 MeV energy range based on an improved dielectric response model. A new *I*-value for liquid water is determined while the importance of including non-RPA effects into the momentum dependence of the dielectric function is explicitly investigated. The magnitude of low-energy corrections to the Born approximation is also examined.

2. Method

2.1. The Born approximation

The electronic (or collision) stopping power (S_{col}) of a material for a charged projectile represents its mean energy loss per unit path length due to inelastic Coulomb collisions with target electrons and is formally obtained from the differential-in-energy-transfer inelastic cross section as follows (ICRU 1993):

$$S_{col} = \int_0^{E_{max}} E \frac{d\Lambda}{dE} \, dE, \tag{1}$$

where Λ is the macroscopic inelastic cross section (or inverse inelastic mean free path) and E is the energy transfer from the projectile to the target electrons leading to ionization and/or (discrete) excitation events. In the latter case, the integration must be replaced by a summation over the allowed discrete electronic transitions (for simplicity, we keep here the more general notation). For protons the upper limit of integration is $E_{max} \approx 4T$ where $T = m\upsilon^2/2$ or $T = (m/M)\tau$ with m the electron rest mass ($mc^2 = 511$ keV), and υ, τ and M are the proton velocity, kinetic energy and rest mass ($Mc^2 = 938$ MeV), respectively. The restricted stopping power (S_Δ) can be directly obtained from equation (1) by simply replacing E_{max} by some fixed cut-off value Δ for the maximum energy transfer in inelastic collisions ($\Delta \leqslant E_{max}$).

Assuming sufficiently fast (but still non-relativistic) projectiles of fixed charge so that the plane wave Born approximation (PWBA) is valid, the dielectric description of Λ for an isotropic and homogeneous medium (so that the momentum transfer q is scalar) leads to the following expression for the electronic stopping power (Ritchie 1982):

$$S_{Born} = \frac{z^2}{\pi a_0 T} \int_0^{E_{max}} E \, dE \int_{q_{min}}^{q_{max}} \frac{1}{q} Im[-1/\varepsilon(E, q)] \, dq, \tag{2}$$

where $a_0 = \hbar/(me^2)$ is the Bohr radius ($a_0 = 0.529 \times 10^{-10}$ m), z is the projectile charge, Im[ ] denotes the imaginary part of the argument and $\varepsilon(E, q) = \varepsilon_1(E, q) + i\varepsilon_2(E, q)$ is the target dielectric response function, which contains all the dynamic properties of the material related to its response to an external perturbation (e.g. charged particle beam). The limits of integration over q in equation (2) are $q_{max/min} = \sqrt{2M}(\sqrt{\tau} \pm \sqrt{\tau - E})$. It follows from equation (2) that the imaginary part of the inverse dielectric function, $Im[-1/\varepsilon(E, q)]$, the so-called target energy-loss function (ELF), is the fundamental material property within PWBA. It should be highlighted that in order to calculate the electronic stopping power according to equation (2), the ELF must be known over the whole energy–momentum plane; this is the so-called Bethe surface of the material (Inokuti 1971). Presently, a numerical evaluation of the Bethe surface of a liquid or amorphous solid is not feasible, and even for simple molecules some drastic approximations need to be made (Segui *et al* 2002).

2.2. Dielectric response function

The construction of the model dielectric response function $\varepsilon(E, q)$ for liquid water used in the present study follows the Ritchie–Howie methodology and has been presented in detail elsewhere (Emfietzoglou *et al* 2005). Here, we will provide a summary of the model, discuss an improved K-shell calculation and highlight those aspects which are pertinent to the present study and set it apart from previous similar calculations. In particular, the inclusion of non-RPA effects in the extension of the dielectric function to finite momentum transfer will be discussed in some detail in order to reveal the deficiencies of some widely used schemes. The basis of our model is the following Drude-like dielectric function:

$$\varepsilon(E, q) = 1 + f_j(q)E_p^2\{E_j^2(q) - E^2 - iE\gamma_j(q)\}^{-1}, \tag{3}$$

where E_p is a nominal plasmon energy of the material determined from the relationship $E_p = 4\sqrt{n\pi a_0^3}$ Ry, where n is the electronic density and Ry = 13.6 eV. For liquid water of mass density of 1 g cm^{-3}, $n = 3.34 \times 10^{23}$ cm^{-3} so $E_p = 21.4$ eV. The triad of values $\{E_j, \gamma_j, f_j\}$ in equation (3) are associated with the energy, lifetime and strength, respectively, of the jth electronic transition. Assuming a one-mode excitation spectrum ($j = 1$ and $f_j = 1$) and interpreting $E_j(q = 0)$ as an effective band gap, equation (3) becomes identical to the original Ritchie–Howie dielectric function as applied to non-metals (i.e. semiconductors and

insulators). Also, for free-electron materials ($E_j = 0$ and $f_j = 1$), equation (3) coincides with the original Drude dielectric function at the limit $q \to 0$; thus, equation (3) generalizes the Drude function to all materials and provides its extension to non-zero q values (it is therefore often called an extended-Drude dielectric function). The procedure to determine equation (3) will be divided into two parts, namely the one pertaining to its optical limit ($q \to 0$) and the other to its extension to finite momentum transfer ($q > 0$).

2.2.1. Optical limit. With respect to the optical limit, equation (3) is used to analytically fit the most recent dielectric data of liquid water obtained from inelastic x-ray scattering spectroscopy (IXSS) (Hayashi *et al* 2000). The IXSS data extend from 6 to 160 eV providing a near complete knowledge of the dielectric response properties of the valence shells ('v') of liquid water through $\varepsilon_1^v(E, 0), \varepsilon_2^v(E, 0)$ and $\mathrm{Im}[-1/\varepsilon^v(E, 0)]$. Overall, five discrete excitations (A^1B_1, B^1A_1, Ryd A + B, Ryd C + D and diffuse bands) and four ionization shells ($1b_1$, $3a_1$, $1b_2$, $2a_1$) were considered in the deconvolution of the IXSS data for $\varepsilon_2^v(E, 0)$. As also found by others (Dingfelder *et al* 1998), the fitting of the low-energy part of the spectrum is substantially improved if derivative Drude functions (which are more sharply peaked) are used for the five discrete excitation levels. Ionization thresholds were set at 10, 13, 17 and 32 eV whereas excitation energies were distributed between 8 and 15 eV with a threshold (or energy gap) at 7 eV. This is a working 'energy-band' model for liquid water in line with recent experiments (Wilson *et al* 2001, Winter *et al* 2004). For the K-shell, we use here the hydrogenic GOS approximation, $\mathrm{d}f^K(E, q)/\mathrm{d}E$ (Dingfelder *et al* 2000, Heredia-Avalos *et al* 2005, Garcia-Molina *et al* 2009), which improves the asymptotic behavior of the Drude function used earlier (Emfietzoglou *et al* 2005). The latter was based on the photoabsorption cross sections, σ_{ph}^K, of the NIST-FFAST database (Chantler *et al* 2005). The two quantities are related through $\mathrm{d}f^K(E, 0)/\mathrm{d}E = \left(4\pi^2\alpha^2 a_0^2 \mathrm{Ry}\right)^{-1}\sigma_{ph}^K$ where $\alpha = 1/137$. In both cases, it is assumed that due to the large difference between the K-edge ($\sim$540 eV) and the valence excitation region ($<$100 eV), the former retains its atomic character so that the approximate relation $\mathrm{Im}(-1/\varepsilon^K) \approx \varepsilon_2^K$ holds. After combining the valence and K-shell contribution, our optical-ELF (OELF) of liquid water is obtained from

$$\mathrm{Im}[-1/\varepsilon(E, 0)] = \mathrm{Im}[-1/\varepsilon^v(E, 0)] + \varepsilon_2^K(E, 0), \tag{4}$$

where $\varepsilon_2^K(E, 0) = \left(\pi E_p^2/2Z\right) \times E^{-1}\mathrm{d}f^K(E, 0)/\mathrm{d}E$, with Z being the number of electrons in the water molecule.

To a large extent, the general characteristics of our optical-data model are also shared by earlier dielectric response models of liquid water, most notably, by the ORNL (Ritchie *et al* 1991) and GSF (Dingfelder *et al* 1998, 2000) models which have been documented in sufficient detail. An important difference, however, is that all earlier models are based on the old optical reflectance data of Heller *et al* (1974) whereas the present model is based on the more recent IXSS data of Hayashi *et al* (2000). It has been shown recently that this change alone has a sizeable impact on both electron and proton inelastic calculations (Emfietzoglou and Nikjoo 2005, 2007, Emfietzoglou *et al* 2006a, 2006b).

An independent test for the overall consistency of a dielectric optical-data model is provided by the following sum rules (Smith *et al* 2006):

$$f \text{ sum rule} : \frac{2}{\pi E_p^2} \int_0^\infty E \, \mathrm{Im}[-1/\varepsilon(E, 0)] \, \mathrm{d}E = 1, \tag{5a}$$

$$\text{conductivity sum rule} : \frac{2}{\pi E_p^2} \int_0^\infty E \, \mathrm{Im}[\varepsilon(E, 0)] \, \mathrm{d}E = 1, \tag{5b}$$

perfect screening sum rule : $\dfrac{2}{\pi} \displaystyle\int_0^\infty \dfrac{1}{E} \, \mathrm{Im}[-1/\varepsilon(E, 0)] \, \mathrm{d}E + \mathrm{Re}[1/\varepsilon(0, 0)] = 1.$ (5c)

In the present case, all the above sum rules were satisfied to better than 1% (see section 3).

2.2.2. Momentum extension: random phase approximation (RPA). The extension of the optical dielectric function $\varepsilon(E, 0)$ to finite momentum transfer ($q > 0$) is obtained following the Ritchie–Howie approach where the momentum dependence is introduced through appropriate dispersion relations for the Drude coefficients. The search for a physically motivated extension scheme can be guided by the observation that at $q = 0$ (and $E \approx E_p$), the Drude dielectric function with $\gamma = 0$ coincides with the Lindhard (RPA) dielectric function which, for small q, exhibits the dispersion relation $E_p(q) = E_p + \alpha_{\mathrm{RPA}}(q^2/2m)$ where $\alpha_{\mathrm{RPA}} = (6E_F/5E_p)$. For liquid water, the free-electron values of the Fermi (E_F) and plasmon (E_p) energies are 17.5 eV and 21.4 eV, respectively, so the RPA coefficient is about unity ($\alpha_{\mathrm{RPA}} = 0.981$). Then, the widely used quadratic dispersion for the Drude energy coefficient follows:

$$E_j(q) = E_j + \left(\frac{q^2}{2m}\right). \tag{6}$$

Despite its simplicity, equation (6) is adequate for sufficiently fast projectiles by virtue of its correct limiting form at $q \to 0$ and $q \to \infty$ (Fernandez-Varea *et al* 1992, 1993). The latter ensures that, at high q, single-particle effects are accounted for in an approximate manner by a quadratic kinetic term, $q^2/2m$, that represents a free-electron-like response. The above quadratic dispersion leads to the characteristic Bethe ridge (Dingfelder and Inokuti 1999). For not too fast projectiles (e.g. the Bragg peak region), however, improvements upon the quadratic RPA dispersion must be considered (Planes *et al* 1996, Ding and Shimizu 1989, 1996, Kuhr and Fitting 1999).

2.2.3. Momentum extension: local field correction (LFC). It is well known from the electron gas (or Fermi liquid) theory that the RPA plasmon dispersion must be corrected downward by the so-called many-body local field correction (LFC) which accounts for short-range exchange-correlation effects not included in RPA (Ichimaru 1982). Using a static (i.e. frequency-independent) approximation to the LFC, the plasmon dispersion for small q now reads

$$E_p(q) = E_p + \alpha_{\mathrm{RPA}} \left\{ 1 - \left(\frac{5E_p^2}{12E_F^2} \right) \mathrm{A_{LFC}} \right\} \left(\frac{q^2}{2m} \right), \tag{7}$$

where $\mathrm{A_{LFC}} = (q_F/q)^2 G(q \to 0)$ with $G(q \to 0)$ being the static-LFC at the long wavelength limit. In the context of an extended optical-data dielectric model, an LFC is applied somewhat indirectly by treating the quadratic RPA coefficient as an adjustable parameter (Kuhr and Fitting 1999). For liquid water, it is only recently that Emfietzoglou *et al* (2005) first considered such a correction to the RPA dispersion. These authors found that to better represent the IXSS data of Watanabe *et al* (1997, 2000) over the momentum transfer range: $0.69 < q < 3.59$ atomic units (a.u.), the following dispersion relation must be used:

$$E_j(q) = E_j + g(q) \left(\frac{q^2}{2m} \right), \tag{8}$$

where $\mathrm{g}(q) = 1 - \exp(-c\,q^d)$, with the empirically determined parameters $c = 1.5$ and $d = 0.4$ (q in a.u). Contrary to equation (7), which is strictly correct for small q, equation (8)

is made applicable for all q by using a q-dependent correction which has the desired limiting behavior, i.e. $g(q \to 0) = 0$ and $g(q \to \infty) = 1$. The latter ensures that single-particle effects are still accounted for by the quadratic term characteristic of a free-electron-like response.

2.2.4. Momentum extension: damping. Within Lindhard's theory, plasmons are undamped electronic excitations (i.e. have infinite lifetime or zero linewidth) up to a critical wavevector where they decay to electron-hole pairs. Such a sharply peaked ELF spectrum is in contrast to a large body of experimental evidence that indicate a strong damping mechanism at all q for most materials (Sturm 1982). Mermin (1970) has provided a phenomenological modification to the Lindhard dielectric function that includes plasmon damping by phonon-assisted electronic transitions. Plasmon decay through two (or more) electron–hole pairs has been investigated extensively and it is a natural outcome in the context of a dynamic (i.e. frequency-dependent) LFC (Sturm and Gusarov 2000). The important point is that, for small q, all studies predict a quadratic dispersion for plasmon damping: $\gamma(q) \propto bq^2$, differing only in the magnitude (and nature) of the q^2-coefficient (Bachlechner *et al* 1991, 1993). The q-dependence of $\gamma_j(q)$ and the associated momentum broadening of the ELF have been considered in several extended optical-data dielectric models to various degrees of sophistication (Ding and Shimizu 1989, 1996, Planes *et al* 1996, Abril *et al* 1998, Kuhr and Fitting 1999). In contrast, the effect of momentum broadening on the Bethe ridge of liquid water was first considered only recently by Emfietzoglou *et al* (2005, 2008) who used both a linear and a quadratic dispersion term to properly represent the IXSS data:

$$\gamma_j(q) = \gamma_j + aq + bq^2, \tag{9}$$

where the values of the coefficients are $a = 10$ eV and $b = 6$ eV (q in a.u.). Recently, a revision of the ORNL dielectric model was reported where a linear dispersion for the damping coefficient was used in the form $\gamma_j(q) = \gamma_j + q$Ry (Dingfelder *et al* 2008).

2.2.5. Momentum extension: the plasmon-pole approximation. A convenient simplification of the Lindhard dielectric function is the so-called plasmon-pole approximation, which replaces the entire ELF spectrum by a single plasmon excitation along the dispersion line $E_p(q)$ (Overhauser 1971, Penn 1976). Its utility in the context of the extended optical-data methodology was revealed by the pioneering work of Penn (1987), which served as the basis of the widely used Tanuma–Powell–Penn calculations of electron inelastic mean free paths (Tanuma *et al* 2003) and stopping powers (Tanuma *et al* 2008) in solids. The first application of the plasmon-pole approximation to proton stopping was done by Ashley (1991). More recently, Akkerman *et al* (2001) and Tan *et al* (2006, 2008) have used it to calculate proton stopping powers in a variety of biological compounds including liquid water. The form of the plasmon-pole dielectric function follows from equation (3) if we assume that collective (plasmon-like) excitations take place at resonance energies $\Omega_0^2 = E_j^2 + E_p^2$ with zero damping ($\gamma \to 0$). Then, it may be shown that the momentum-dependent ELF can be obtained from its optical limit through (Penn 1987):

$$\text{Im}[-1/\varepsilon(E,q)] = \frac{E_o}{E} \text{Im}[-1/\varepsilon(E_o, q = 0)], \tag{10}$$

where E_o is the positive solution of the dispersion relationship $E_p(E_o, q) = E$. To our knowledge, all calculations so far within this scheme for proton stopping have followed Ashley (1991) and used the quadratic RPA dispersion relation (equation (6)). Alternatively, as suggested by Penn (1976, 1987), one can adopt the more accurate expression:

$$E_p^2(q) = E_p^2 + (4/3) E_F \left(\frac{q^2}{2m} \right) + \left(\frac{q^2}{2m} \right)^2. \tag{11}$$

2.3. The Bethe approximation

By using the *f* sum rule and a distinction between low- and high-*q* collisions, Bethe showed that equation (2) reduces to the following asymptotic form in powers of $1/T$ (Inokuti 1971):

$$S = AT^{-1}\ln(T) + BT^{-1} + CT^{-2} + \cdots. \tag{12}$$

Since the Born approximation is essentially a high-*T* approximation, equation (12) automatically provides the most important contributions to the stopping power. Specifically, the terms of order T^{-1} will be dominant at high energies, whereas the term of order T^{-2} provides the principal correction at lower energies. The coefficients *A*, *B* and *C* depend on target properties related to the ELF. Importantly, the coefficients *A* and *B* of the first-order terms (T^{-1}) are obtained solely from the optical limit of the ELF:

$$A = \frac{E_p^2}{2a_0}, \tag{13}$$

$$B = A\ln\left(\frac{4}{I}\right), \tag{14}$$

where *I* is the mean excitation energy which, for condensed systems, is defined by

$$\ln(I) = \frac{\int_0^\infty E\ln(E)\mathrm{Im}[-1/\varepsilon(E,0)]\,\mathrm{d}E}{\int_0^\infty E\,\mathrm{Im}[-1/\varepsilon(E,0)]\,\mathrm{d}E}. \tag{15}$$

The leading order of equation (12) constitutes the well-known (uncorrected) Bethe stopping power formula which, for heavy projectiles of charge *z* and coefficients from equations (13)–(15), reads

$$S_{\mathrm{Bethe}} = \frac{z^2 E_p^2}{2a_0 T}\ln\left(\frac{4T}{I}\right). \tag{16}$$

It follows that the Bethe formula, equation (16), is based not only on the Born approximation but also on an additional high-energy approximation in the form of a dipole approximation which assumes that the next order term (CT^{-2}), which depends upon the extension of the ELF to finite momentum transfer, is negligible (Basbas 1984). Thus, low-energy corrections to Bethe's formula of order T^{-2} originate from non-dipole interactions. In the conventional terminology, these represent the so-called shell corrections (C/Z) to Bethe's stopping power formula (the *C* used in the shell-correction term, equations (17) and (18), is related to but different from the one used in equation (12)):

$$S_{\mathrm{full-Bethe}} = \frac{z^2 E_p^2}{2a_0 T}\left[\ln\left(\frac{4T}{I}\right) - \frac{C}{Z}\right]. \tag{17}$$

Fano (1963) has given a theoretical non-relativistic expression for the shell-correction term which, in principle, allows the contribution of each individual shell to be calculated independently. If recast in terms of the ELF, Fano's expression reads

$$\frac{C}{Z} = \frac{C_1}{Z} + \frac{C_2}{Z}, \tag{18a}$$

$$\frac{C_1}{Z} = \frac{2}{\pi E_p^2}\int_0^{E_{\max}} E\,\mathrm{d}E\int_0^{q_{\min}}\frac{1}{q}\left\{\mathrm{Im}\left[-1/\varepsilon(E,q)\right] - \mathrm{Im}\left[-1/\varepsilon(E,0)\right]\right\}\mathrm{d}q, \tag{18b}$$

$$\frac{C_2}{Z} = -\frac{2}{\pi E_p^2}\int_0^{E_{\max}} E\,\mathrm{d}E\int_{q_{\max}}^{\infty}\frac{1}{q}\,\mathrm{Im}[-1/\varepsilon(E,q)]\,\mathrm{d}q. \tag{18c}$$

Since $q_{min} \approx E/\upsilon$, the shell-correction term increases with decreasing projectile velocity and is more important for inner shells than for outer shells by virtue of their larger binding energies (and thus the energy loss E). An alternative and perhaps more practical definition of the shell-correction term is based on the following relation (Oddershede *et al* 2005, Sigmund and Schinner 2006):

$$\frac{C}{Z} = L_{Bethe} - L_{Born}, \tag{19}$$

where

$$L_{Bethe} = \ln\left(\frac{4T}{I}\right) \tag{20}$$

and

$$L_{Born} = \frac{2a_0 T}{z^2 E_p^2} S_{Born}. \tag{21}$$

In the present work, shell-correction calculations by both the above approaches are presented.

2.4. Low-energy Born corrections

2.4.1. Barkas and Bloch terms. As the projectile velocity decreases, first-order perturbation theory is inadequate and higher order terms proportional to z^3 and z^4 must be included to account, respectively, for the Barkas effect and the Bloch correction term. The corrected stopping power then reads

$$S_{corrected} = S_{Born} + S_{Barkas} + S_{Bloch} \tag{22}$$

or

$$S_{corrected} = \frac{z^2 E_p^2}{2a_0 T}(L_{full-Bethe} + z L_{Barkas} + z^2 L_{Bloch}), \tag{23}$$

where $L_{full-Bethe}$ is the stopping number, the term between brackets in equation (17), which includes the shell-correction term.

Although a generally accepted theory of the Barkas effect is not available, the Ashley–Ritchie–Brandt (ARB) statistical model (Ashley *et al* 1972, 1973) has appeared over the years to offer the most practical approach for representing the Barkas-effect correction to stopping theory (Porter and Lin 1990, ICRU 1993). More recently, Ashley (1991) has suggested an improvement to the ARB model in those cases where the actual absorption spectrum of the material is known. Then, in the 'distant collision' (or optical) approximation of the Barkas effect, the corresponding stopping number reads (Ashley 1991)

$$L_{Barkas} = \frac{2}{\pi E_p^2} \int_0^{E_{max}} E \, \text{Im}\left[-1/\varepsilon(E, 0)\right] L_1(E; \xi) \, dE, \tag{24}$$

where

$$L_1(E; \xi) = (\sqrt{Ry}/2)\frac{E}{T^{3/2}}H(\xi), \tag{25}$$

with $\xi = 0.1356a(E/T^{1/2})$, where a is the minimum distance of glancing collisions, and $H(\xi)$ being a tabulated function which has been analytically approximated by Ashley (1991). For the value of the model parameter a, there are two choices, namely the Jackson and McCarthy (1972) value of $a = 3.688/E^{1/2}$ and the Lindhard (1976) value of $a = 2.070/T^{1/2}$. For organic insulators including liquid water, the Jackson and McCarthy value has been found

(Akkerman *et al* 2001, Emfietzoglou *et al* 2006a) to result in much more reasonable values for the Barkas-effect correction and, therefore, it is adopted here.

For the Bloch correction term, we use the standard parametrization (Bichsel and Porter 1982, ICRU 1993):

$$z^2 L_{\text{Bloch}} = -y^2 \{1.202 - y^2(1.042 - 0.855y^2 + 0.343y^4)\}, \tag{26}$$

where $y = z(\alpha/\beta)$ with $\alpha = 1/137$ and $\beta = \upsilon/c$.

2.4.2. Charge-state effect. At projectile energies in the region of the stopping maximum and below, the process of charge exchange between the projectile and the target (i.e. electron capture from and loss to the target) modifies the energy loss as calculated from equation (2). At dynamic equilibrium, we can assign a particular charge fraction at each charge state of the projectile in the material. Then, the electronic stopping power can be obtained by a weighted sum of the electronic stopping power for each charge state k of the projectile (Heredia-Avalos and Garcia-Molina 2002):

$$S = \sum_{k=0}^{z} \phi_k S_k, \tag{27}$$

where ϕ_k is the probability of finding the projectile in a given charge state k. The ϕ_k values, assuming that they equal the charge-state fractions at equilibrium, will depend upon the target material, the projectile and its velocity. In the present work, ϕ_k are obtained from the CasP 3.1 code (Grande and Schiwietz 2005). Then, the electronic stopping power in the Born approximation for a projectile with charge-state k is given, instead of equation (2), by (Ferrell and Ritchie 1977)

$$S_{\text{Born},k} = \frac{z^2}{\pi a_0 T} \int_0^{E_{\text{max}}} E \, dE \int_{q_{\text{min}}}^{q_{\text{max}}} \frac{\rho_k^2(q)}{q} \, \text{Im}[-1/\varepsilon(E, q)] \, dq, \tag{28}$$

where $\rho_k(q)$ is the Fourier transform of the projectile charge density for the charge-state k. In the present study, $\rho_k(q)$ is calculated according to the modified Brandt–Kitagawa model (Brandt and Kitagawa 1982, Brandt 1982) which has been successfully applied for proton stopping in various solids (Garcia-Molina *et al* 2006).

3. Results

Our optical energy-loss function (OELF) based on equation (4) is presented in figure 1 along with the most recent data for water. The IXSS data (Hayashi *et al* 2000) pertain to the valence shells of the *liquid phase* covering the energy range from 6 to 160 eV. On the other hand, the data from the FFAST database of NIST refer to the water molecule in the *gas phase* including the oxygen K-shell which sets in at $\sim$540 eV. The total OELF is shown for two different representations of the K-shell, namely a Drude function parametrization (Emfietzoglou *et al* 2005) and a hydrogenic GOS (Heredia-Avalos *et al* 2005, Garcia-Molina *et al* 2009) assuming in both cases that $\text{Im}(-1/\varepsilon^K) \approx \varepsilon_2^K$. The sum rules calculated from equations (5a), (5b) and (5c) give 1.00 (f sum rule), 0.998 (conductivity sum rule) and 1.01 (perfect screening sum rule), respectively. For the latter, we have used the relationship $\text{Re}[1/\varepsilon(0,0)] = 1/\varepsilon_1(0,0) = 1/n^2$, where $n = 0.572$ is the refractive index of liquid water taken from Hayashi *et al* (2000). The contribution of the oxygen K-shell to the OELF is explicitly shown in figure 2. For both the Drude and hydrogenic representations, the K-shell contribution to the f sum rule was fixed at 0.179 consistent with accurate atomic calculations (Inokuti *et al* 1981).
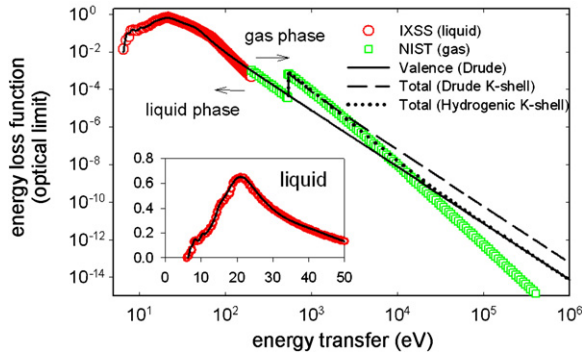
Figure 1. Our ELF model for water at the optical limit (equation (4)) is compared to the inelastic x-ray scattering spectroscopy (IXSS) measurements of Hayashi *et al* (2000) for liquid water, and the FFAST database of NIST (Chantler *et al* 2005) for the water molecule. The total ELF is shown for two different representations of the K-shell, namely a Drude parametrization or a hydrogenic GOS, assuming in both cases that $\text{Im}(-1/\varepsilon^K) \approx \varepsilon_2^K$. In the inset, we focus on the valence losses of liquid water and compare our model with the IXSS data.
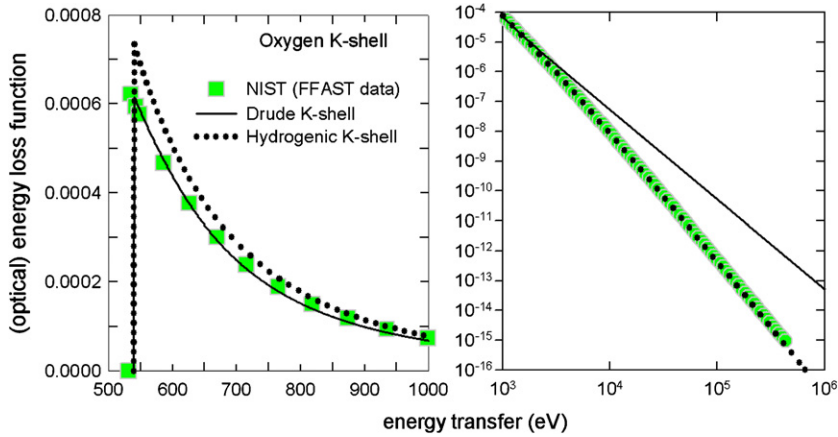
Figure 2. Similar to figure 1, for the K-shell only.

The mean excitation energy (*I*-value) of liquid water calculated from equation (15) but with a variable maximum energy transfer is presented in figure 3. Similar to figure 1, the total *I*-value is also shown for two different representations of the K-shell, namely a Drude function parametrization (Emfietzoglou *et al* 2005) and a hydrogenic GOS (Heredia-Avalos *et al* 2005, Garcia-Molina *et al* 2009). The use of a Drude K-shell leads to $I = 82.4$ eV whereas a hydrogenic K-shell to $I = 77.8$ eV. Further increase in the maximum energy transfer beyond 1 MeV does not alter the above values to the third significant digit.

The momentum dependence of the ELF using both the plasmon-pole approximation (equation (10)) and the extended-Drude dielectric function (equation (3)) is presented in figure 4. Note that all ELF models coincide at the optical limit ($q = 0$) where the OELF of figure 1 is obtained. Comparisons are made against the IXSS data (Watanabe *et al* 1997, 2000) for momentum transfer values $q = 1.02$, 1.81, 2.52 and 3.59 a.u. For the plasmon-pole calculations, we use the dispersion schemes suggested by Ashley (1991) and Penn (1987). The former employs the quadratic RPA dispersion (equation (6)) whereas the latter
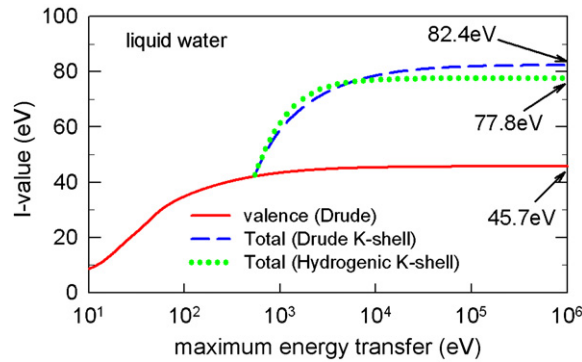
Figure 3. The mean excitation energy (*I*) of the stopping power theory is calculated as a function of the maximum energy transfer from equation (15). The contribution of the K-shell is calculated by both a Drude parametrization and a hydrogenic GOS (see figures 1 and 2).
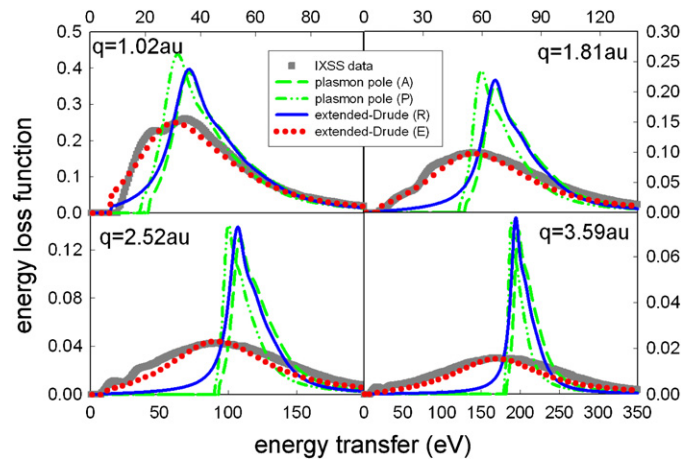

Figure 4. Comparison of IXSS data (Watanabe *et al* 1997, 2000) for the ELF of liquid water at finite momentum-transfer ($q > 0$) with calculations based on extended optical-data dielectric response models having different dispersion schemes (see the text for explanation on the models; P: Penn, A: Ashley, R: Ritchie, E: Emfietzoglou).

uses an improved expression (equation (11)). For the extended-Drude calculations, we use both the quadratic RPA dispersion (equation (6)) suggested by Ritchie *et al* (1991) and the corrected RPA dispersion of Emfietzoglou *et al* (2005), which accounts for local field effects by equation (8) and damping by equation (9). Note that the energy range depicted is below the K-edge so there is only contribution from the valence shells.

The above dielectric response models are then used to calculate in the Born approximation (equation (2)) the electronic stopping power of liquid water for energetic protons (figure 5). The Bethe approximation calculated from equation (16) with $I = 75$ eV (ICRU 1984, 1993) is also shown for comparison.

A comparison of theoretical and experimental data on the electronic stopping power of water in the condensed phase (liquid water or water ice) is presented in figure 6. Values are shown above 50 keV where the electronic stopping is the dominant (but not the only) mechanism of energy loss. The present calculations are based on the charge-state
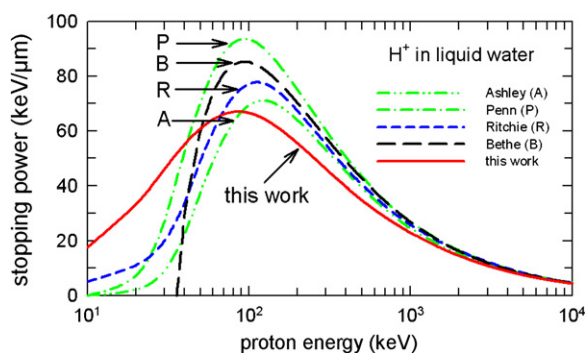
Figure 5. The electronic stopping power of liquid water in the Born approximation as a function of proton energy calculated by different dielectric response models (see the text for explanation of models). Results from the (uncorrected) Bethe formula with an *I*-value of 75 eV (ICRU 1984, 1993) are depicted for comparison.
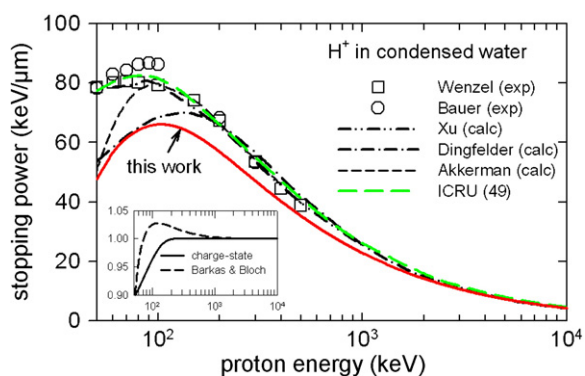

Figure 6. Comparison of our present calculations of the electronic stopping power of liquid water (corrected for Barkas, Bloch, and charge state) with the ICRU (1993) values and other theoretical and experimental studies. The data of Wenzel and Whaling (1952) and Bauer *et al* (1998) are based on experimental measurements on D_2O-ice and H_2O-ice, respectively, while the calculations of Xu *et al* (1985), Dingfelder *et al* (2000) and Akkerman *et al* (2001) use different approximations for the dielectric response function of liquid water (see the text). In the inset, we plot the ratio of the Barkas–Bloch (equation (22)) and charge state (equation (28)) corrected stopping power to the uncorrected (Born) stopping power (equation (2)).

approximation (equations (27) and (28)) supplemented with Barkas and Bloch terms (equations (24)–(26)). The ELF is obtained from the present dielectric response model (equations (3), (4), (8) and (9)) which combines the corrected RPA dielectric response model of Emfietzoglou *et al* (2005) for the valence shells and the hydrogenic GOS for the K-shell. In the inset, we show the ratio of the Barkas–Bloch (equation (22)) and charge-state (equation (28)) corrected stopping power to the uncorrected (Born) stopping power (equation (2)). The use of a charge-state correction is responsible for the slightly lower stopping power values in the region of the maximum compared to those of Emfietzoglou *et al* (2007a) which employ the same dielectric function for the valence shells with the present study. The calculations by Dingfelder *et al* (2000) and Akkerman *et al* (2001) use the extended-Drude and plasmon-pole approximations, respectively, with a quadratic RPA dispersion (equation (6)). However, the optical limit in both studies is constructed based on a parametrization of the old reflectance
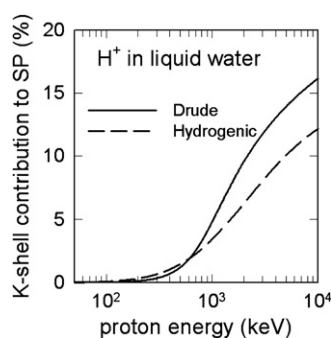
Figure 7. The K-shell contribution (in%) to the total electronic stopping power as a function of proton energy calculated by the hydrogenic GOS model and the extended-Drude model with the corrected RPA dispersion.

data of Heller *et al* (1974). The calculations of Xu *et al* (1985) are based on a modified local-plasma approximation model. The data of Wenzel and Whaling (1952) and Bauer *et al* (1998) are based on experimental measurements on D_2O–ice and H_2O–ice, respectively, with reported uncertainties at ∼5%. Finally, for energies above 0.5 MeV, the ICRU (1993) values are based on the Bethe formula (with $I = 75$ eV) supplemented with Barkas, Bloch and shell-correction terms, while at lower energies a fit to experimental data is being used; note that these experimental data correspond to ice and not liquid water. The contribution of the K-shell to the total electronic stopping over the above energy range is shown in figure 7. This contribution is calculated based on either a hydrogenic GOS or the extended-Drude model with the corrected RPA dispersion.

The shell-correction term (C/Z) defined as the difference between the Bethe and Born stopping numbers (equation (19)) is depicted in figure 8 (panel a) for two different values of the mean excitation energy, while the ratio $(C/Z)/L_{Born}$ is shown in the inset. In panel b, Fano's expression for C/Z (equation (18)) has been used to calculate, based on the different dielectric response models discussed above (see figure 4), the separate contribution of the valence and K-shell to the (total) shell-correction term.

The magnitude of the various stopping numbers (L) is presented in figure 9. The Born stopping number (L_{Born}) corresponds to the present dielectric response model, the Barkas (L_{Barkas}) and Bloch ($-L_{Bloch}$) stopping numbers are evaluated according to equations (24) to (26), and the Bethe stopping number (L_{Bethe}) represents the logarithmic term in Bethe's formula (equations (16) and (20)) for $I = 75$ eV.

Finally, in figure 10, we present the ratio of the restricted to the total electronic stopping power over the proton energy range from 0.5 to 10 MeV for different cut-off values of maximum energy transfer. The ICRU (1993) values are compared with those obtained from the present dielectric response model.

4. Discussion

4.1. The I-value of liquid water

The mean excitation energy (the so-called *I*-value) is the most important material quantity in the calculation of the electronic stopping power of energetic ions (>1 MeV u^{-1}) through Bethe's formula and represents its main source of uncertainty at high energies (Kamakura *et al* 2006). The *I*-value can be generally determined in three ways: (i) from an analysis
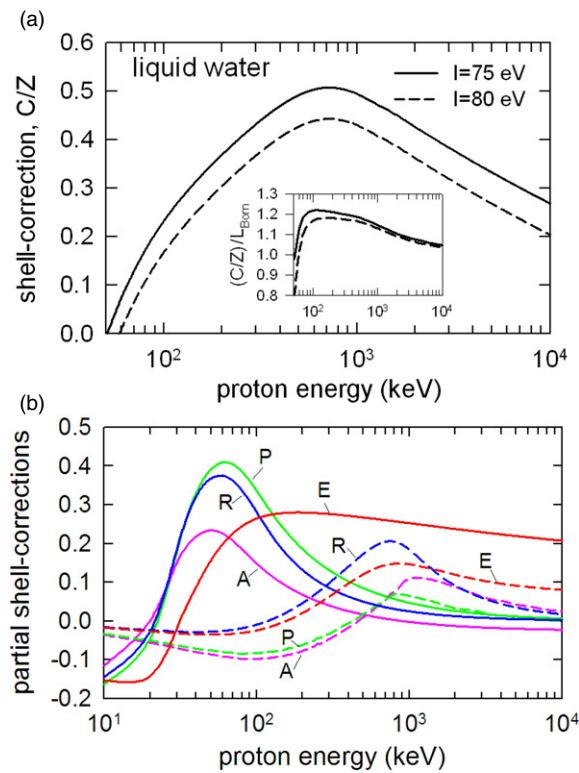
Figure 8. (a) The shell-correction term (C/Z) calculated from the present dielectric response model using the difference between the Bethe and Born stopping numbers (equation (19)) for two different values of the mean excitation energy. The inset presents the ratio of $(C/Z)/L_{Born}$. (b) Fano's expression for C/Z (equation (18)) is used to calculate partial shell corrections for the valence (full-line) and K-shell (broken-line) based on dielectric response models having different dispersions but the same optical limit (see the text for explanation on the models; P: Penn, A: Ashley, R: Ritchie, E: Emfietzoglou).
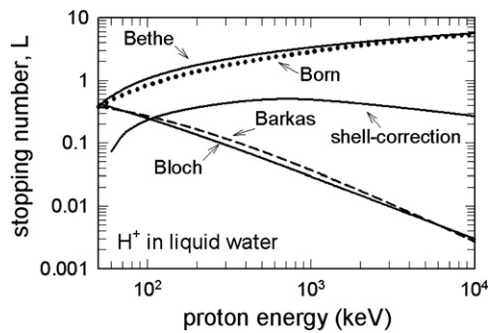

Figure 9. The various stopping numbers (L) corresponding to the present dielectric response model (L_{Born}; having $I = 77.8$ eV), the Barkas (L_{Barkas}) and Bloch ($-L_{Bloch}$) corrections evaluated from equations (24) to (26), and the Bethe stopping number (L_{Bethe}) of equation (20) for $I = 75$ eV.
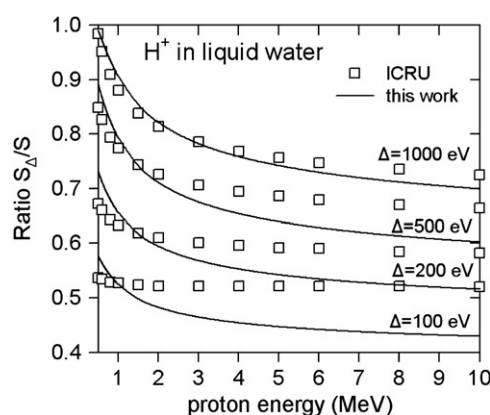
Figure 10. The ratio of the restricted (S_Δ) to the total (S) electronic stopping power over the proton energy range from 0.5 to 10 MeV, for different cut-off values of maximum energy transfer (Δ); comparison of the ICRU (1993) values with those obtained from the present dielectric response model.

of stopping power (and range) measurements, (ii) from optical absorption data and (iii) by *ab initio* calculations. The last method is not yet applicable to condensed targets (liquids and solids). Recently, Paul (Paul 2007a, 2007b, Paul *et al* 2007a, 2007b) has reviewed the literature on the *I*-value of liquid water and concluded that an *I*-value of 80.8 ± 2 eV (Paul *et al* 2007a, 2007b) appears more in line with recent data than the ICRU (1984, 1993) value of 75 ± 3 eV. In the present study, we improve upon our previous semi-empirical estimate of the *I*-value of liquid water (Emfietzoglou *et al* 2005) by a more careful examination of its high-energy (asymptotic) trend and K-shell contribution. The calculations are based on equation (15) which defines the *I*-value as a weighted average over the complete OELF $\mathrm{Im}[-1/\varepsilon(E, q = 0)]$ of the material. The OELF is evaluated semi-empirically from a dielectric response function for the valence shells and an optical oscillator strength for the K-shell. This is a standard methodology for condensed targets, first applied to liquid water by Ritchie *et al* (1978) who obtained an *I*-value of 75 eV. Subsequent studies along the same line by Ashley (1982) and LaVerne and Mozumder (1986) practically confirmed Ritchie's earlier estimate, resulting in 75.4 eV and 74.9 eV, respectively. However, a substantial spread has been observed in more recent calculations: 81.8 eV (Dingfelder *et al* 1998), 74 eV (Akkerman and Akkerman 1999), 72.5 eV (Tan *et al* 2004), 82.4 eV (Emfietzoglou *et al* 2005) and 79.4 eV (Garcia-Molina *et al* 2009). Experiments, on the other hand, have resulted in *I*-values of 74 eV (Luo *et al* 1991), 79.7 ± 0.5 eV (Bichsel and Hiraoka 1992), 77 eV (Kramer *et al* 2000) and, more recently, 78.4 ± 1.0 eV (Kumazaki *et al* 2007). Thus, apart from the study of Luo *et al* (1991), the experimentally determined values clearly point to an upward shift of the ICRU value by a few eV. The situation, however, is less clear with respect to semi-empirical calculations mentioned above. Although the general principles of this approach are well understood and to a good approximation valid, the choice of the data used and the quality of the analytic representation can substantially affect the final outcome. It is important to note that before Emfietzoglou *et al* (2005), nearly all studies despite being based on the same set of dielectric data (Heller *et al* 1974) have resulted in considerably different *I*-values. Furthermore, as reported by Emfietzoglou *et al* (2005), a variation of several eV is expected simply from the choice of the dielectric and/or K-shell data used. These authors first employed the new dielectric data of Hayashi *et al* (2000) which are both more accurate and more complete than the old reflectance data of Heller *et al* (1974), whereas for the K-shell, they used the FFAST database of NIST

which, contrary to the perhaps more familiar XCOM database (also of NIST), extends down to the K-edge (the two databases practically coincide at high energies for water).

The Emfietzoglou *et al* (2005) *I*-value estimate, however, suffers from well-known incorrect asymptotic behavior of the Drude function as clearly shown in figures 1 and 2 (see also the discussion below). To investigate the consequences of the above fact, we have calculated the contribution of the valence and K-shells to the *I*-value as a function of the upper limit of integration in equation (15), i.e. the maximum energy transfer, using both a Drude and a hydrogenic representation for the K-shell (figure 3). For all practical purposes, the *I*-value does not change if the integration is extended beyond $\sim$1 MeV. The K-shell contribution amounts to nearly 40%, so its proper representation is as critical as that of the valence shells. The use of a hydrogenic K-shell leads to an *I*-value of 77.8 eV which is 4.6 eV smaller than the Emfietzoglou *et al* (2005) value of 82.4 eV. Given that the f sum rule contribution of the K-shell was kept fixed (at $f^{\mathrm{K}} = 0.179$) for both the hydrogenic and Drude representation, their difference is due to their asymptotic behavior: the hydrogenic $\varepsilon_2^{\mathrm{K}}(E, 0)$ falls as $\sim E^{-4.5}$ and fits well the NIST data (except near the edge), whereas the Drude $\varepsilon_2^{\mathrm{K}}(E, 0)$ falls as $\sim E^{-3}$ overestimating the data above a few keV. However, as can be clearly seen in figure 1, the improvement brought about by a hydrogenic K-shell is to some extent compromised by the still wrong asymptotic behavior of the Drude valence shells. Thus, the *total* OELF (equation (4)) with a hydrogenic K-shell still overestimates the NIST data above a few tens of keV, albeit to a much smaller extent than a full Drude model. In conclusion, the value of 77.8 eV obtained by the use of the hydrogenic K-shell must be preferred. Its error margin is probably not larger than 1 eV since the hydrogenic curve (see figure 3) has already reached (within 1 eV) its asymptotic value at $\sim$10 keV where the total OELF starts overestimating the data (see figure 1).

4.2. Shell corrections and dispersion effects

Shell corrections represent the most important correction to Bethe's formula below $\sim$1 MeV proton energies. The correction originates from the dipole approximation that leads to the concept of the *I*-value (Basbas 1984). Therefore, they are directly related to the momentum dependence (dispersion) of the dielectric function. Within Bethe's theory, the evaluation of the shell-correction term (C/Z) usually proceeds through equation (19) where the Born stopping number is obtained experimentally. A fundamental problem with this approach is that the shell-correction term becomes important at an energy range where the other low-energy corrections (Barkas and Bloch terms) are sizeable (equation (23)). Moreover, the whole procedure assumes that an accurate *I*-value is already known independently by some other means. As a practical alternative, atomic models for the inner shells and scaling laws for the outer shells are often used in the evaluation of shell corrections (Bichsel 2002). For condensed targets, it is therefore desirable to have an analytic form for the momentum-dependent dielectric response function. As can be seen from figure 8(a), the shell-correction term calculated from the present dielectric response model can reach 20% of L_{Born} at proton energies ($\sim$100 keV) where the electronic stopping power becomes maximum (Bragg peak).

Using Fano's expression, we show in figure 8(b) that the magnitude of the shell-correction term is quite sensitive to the dispersion scheme used and, in particular, to whether damping is included ('E' curve). The latter substantially increases the valence contribution which, in the particular model displayed, exceeds that of the K-shell. In contrast, if damping is neglected, the valence contribution becomes dominant only below a few hundred keV where the K-shell stopping vanishes (figure 7). Note that the results of figure 8(b), although of similar magnitude, do not exactly match those of figure 8(a) and should be considered only

approximate; for example, in all the dielectric models depicted, the K-shell does not satisfy the partial sum rule for *non-zero q* due to the applied large cut-off energy (the K-edge at 540 eV) in the associated Drude function. The present stopping power calculations (figure 6), which use the hydrogenic GOS and not the Drude function representation for the K-shell, are consistent with the shell correction of figure 8(a).

The influence of dispersion upon the magnitude of the electronic stopping power is evident in figure 5. Although differences between the models are only a few percent above 1 MeV, they gradually increase at lower energies reaching 20–30% at 50–100 keV. The reason lies in the different Bethe surface characteristics which directly affect the momentum quadrature over the ELF (Emfietzoglou *et al* 2005, 2008). Specifically, the local-field-type correction used in equation (8) which causes a shift of the ELF to lower energy transfers with increasing q (see figure 4) is responsible for a corresponding shift of the stopping maximum to lower proton energies. On the other hand, the smaller stopping power for energies above the maximum and, especially, the more gradual fall below the maximum are due to damping introduced by equation (9) which causes the momentum broadening of ELF (see figure 4).

The above effects are also responsible for the difference of our present electronic stopping power values and previous calculations by Xu *et al* (1985), Dingfelder *et al* (1998) and Akkerman *et al* (2001) which are all based on a more simplistic dispersion scheme for the momentum dependence of the dielectric function (figure 6). To some extent, they should also be responsible for our differences with ICRU. However, for proton energies below 500 keV where differences are largest, ICRU based its estimates on an empirical fit to experimental data which might include additional stopping mechanisms not examined here (e.g. by charge transfer and by the collisions of neutral hydrogen atoms). Likewise, the neglect in our study of such energy-loss processes might also explain our underestimation by about 20% of the experimental data of Wenzel and Whaling (1952) and Bauer *et al* (1998) which are, however, for ice not liquid water. On the other hand, the differences from ICRU in the restricted stopping power (figure 10) most likely reflect an inherent shortcoming of the ICRU method which employs the Bethe formula with a varied upper limit of binary collisions. As Δ decreases below 1 keV, the Bethe formula grossly overestimates the restricted stopping power. This is because as the upper limit of energy transfer is decreased, the calculation becomes increasingly more sensitive to the exact excitation spectrum of the material (as represented by its ELF) and the use of single parameter (*I*-value) gradually fails.

4.3. Low-energy Born corrections

Higher-order corrections for the Barkas and Bloch effects as well as for the changing charge state of the projectile are known to be important in the region of the stopping maximum and below. From figures 6 (inset) and 9, it is clear that although the Barkas and Bloch terms in absolute terms become sizeable below a few hundred keV, their net effect remains small (<3%) down to 100 keV. At even lower energies, the Bloch term gradually dominates and a net correction of ∼10% is obtained at 50 keV. Similarly, the charge-state correction is relatively insignificant (<3%) above 100 keV, while it increases to ∼10% at 50 keV. Given that the charge-state and the Barkas–Bloch corrections have opposite effects above 100 keV (the former reduces whereas the latter increases the stopping power), their net effect can be safely neglected in that region. On the other hand, below 100 keV the Barkas–Bloch correction turns gradually negative due to the dominance of the latter and adds up to the charge-state correction leading to an ∼20% reduction at 50 keV.

5. Conclusion

The electronic stopping power of liquid water for energetic protons has been studied using an improved dielectric response function. The mean excitation energy (I) of liquid water is estimated to be 77.8 eV with an error margin which is perhaps not larger than 1 eV. The importance of including corrections to the RPA dispersion is shown to have a sizeable impact to shell-correction calculations and to the electronic stopping power at the region of its maximum. Low-energy Born corrections can be safely neglected down to 100 keV proton energies. While our calculated stopping powers satisfactorily agree at high proton energies with currently available tabulations and other calculations, discrepancies appear in the region of the stopping maximum. As these projectile energies determine the development of the Bragg peak, further studies (both theoretical and experimental) in the energy range below 1 MeV would help to elucidate the reported differences.

Acknowledgments

References

Abril I, Garcia-Molina R, Denton C D, Perez-Perez J F and Arista N 1998 Dielectric description of wakes and stopping powers in solids *Phys. Rev.* A **58** 357–66

Akkerman A and Akkerman E 1999 Characteristics of electron inelastic interactions in organic compounds and water over the energy range 20–1000 eV *J. Appl. Phys.* **86** 5809–16

Akkerman A, Breskin A, Chechik R and Lifshitz Y 2001 Calculation of proton stopping power in the region of its maximum value for several organic materials and water *Radiat. Phys. Chem.* **61** 333–5

Ashley J C 1980 Stopping power of an electron gas for slow protons: influence of damping *Nucl. Instrum. Methods* **170** 197–9

Ashley J C 1982 Stopping power of liquid water for low-energy electrons *Radiat. Res.* **89** 25–31

Ashley J C 1991 Optical-data model for the stopping power of condensed matter to protons and antiprotons *J. Phys.: Condens. Matter* **3** 2741–53

Ashley J C, Ritchie R H and Brandt W 1972 Z_1^3 effect in the stopping power of matter for charged particles *Phys. Rev.* B **5** 2393–7

Ashley J C, Ritchie R H and Brandt W 1973 Z_1^3-dependent stopping power and range contributions *Phys. Rev.* A **8** 2402–8

Bachlechner M E, Bohm H M and Schinner A 1993 Screening effects on plasmon damping in an electron liquid *Physica* B **183** 293–302

Bachlechner M E, Macke W, Miesenbock H M and Schinner A 1991 Perturbation analysis of plasmon decay in jellium *Physica* B **168** 104–14

Barriga-Carrasco M D 2008 Mermin dielectric function versus local field corrections on proton stopping in degenerate plasmas *Laser Part. Beams* **26** 389–95

Basbas G 1984 Inner-shell ionization and the Z_1^3 and Barkas effects in stopping power *Nucl. Instrum. Methods* B **4** 227–38

Bauer P, Kaferbock W and Necas V 1998 Investigation of the electronic energy loss of hydrogen ions in H_2O: influence of the state of aggregation *Nucl. Instrum. Methods* B **93** 132–6

Bichsel H 1988 Straggling in thin silicon detectors *Rev. Mod. Phys.* **60** 663–699

Bichsel H 2002 Shell corrections in stopping power *Phys. Rev.* A **65** 052709

Bichsel H and Hiraoka T 1992 Energy loss of 70 MeV protons in elements *Nucl. Instrum. Methods* B **66** 345–51

Bichsel H and Porter L E 1982 Stopping power of protons and alpha particles in H_2, He, N_2, O_2, CH_4, and air *Phys. Rev.* A **25** 2499–510

Brahme A 2004 Recent advances in light ion radiation therapy *Int. J. Radiat. Oncol. Biol. Phys.* **58** 603–16

Brandt W 1982 Effective charges of ions and the stopping power of dense media *Nucl. Instrum. Methods* **194** 13–19

Brandt W and Kitagawa M 1982 Effective stopping-power charges of swift ions in condensed matter *Phys. Rev. B* **25** 5631–7

Chantler C T, Olsen K, Dragoset R A, Kishore A R, Kotochigova S A and Zucker D S 2005 X-ray form factor, attenuation and scattering tables (version 2.1) National Institute of Standards and Technology, Gaithersburg, MD Available at http://physics.nist.gov/ffast

Dabrowski B 1986 Dynamical local-field factor in the response function of an electron gas *Phys. Rev. B* **34** 4989–95

Denton C D, Abril I, Garcia-Molina R, Moreno-Marin C and Heredia-Avalos S 2008 Influence of the description of the target energy-loss function on the energy loss of swift projectiles *Surf. Interface Anal.* **40** 1481–7

Ding Z-J and Shimizu R 1989 Inelastic collisions of kV electrons in solids *Surf. Sci.* **222** 313–31

Ding Z-J and Shimizu R 1996 A Monte Carlo modeling of electron interaction with solids including cascade secondary electron production *Scanning* **18** 92–113

Dingfelder M, Hantke D, Inokuti M and Paretzke H G 1998 Electron inelastic-scattering cross sections in liquid water *Radiat. Phys. Chem.* **53** 1–18

Dingfelder M and Inokuti M 1999 The Bethe surface of liquid water *Radiat. Environ. Biophys.* **38** 93–6

Dingfelder M, Inokuti M and Paretzke H G 2000 Inelastic-collision cross sections of liquid water for interactions of energetic protons *Radiat. Phys. Chem.* **59** 255–75

Dingfelder M, Ritchie R H, Turner J E, Friedland W, Paretzke H G and Hamm R N 2008 Comparisons of calculations with PARTRAC and NOREC: transport of electrons in liquid water *Radiat. Res.* **169** 584–94

Echenique P M, Flores F and Ritchie R H 1990 Dynamic screening of ions in condensed matter *Solid State Phys.* **43** 229–308

Emfietzoglou D, Abril I, Garcia-Molina R, Petsalakis I D, Nikjoo H, Kyriakou I and Pathak A 2008 Semi-empirical dielectric descriptions of the Bethe surface of the valence bands of condensed water *Nucl. Instrum. Methods B* **266** 1154–61

Emfietzoglou D, Cucinotta F and Nikjoo H 2005 A complete dielectric response model for liquid water: a solution of the Bethe ridge problem *Radiat. Res.* **164** 202–11

Emfietzoglou D and Nikjoo H 2005 The effect of model approximations on single-collision distributions of low-energy electrons in liquid water *Radiat. Res.* **163** 98–111

Emfietzoglou D and Nikjoo H 2007 Accurate electron inelastic cross sections and stopping powers for liquid water over the 0.1–10 keV range based on an improved dielectric description of the Bethe surface *Radiat. Res.* **167** 110–20

Emfietzoglou D, Nikjoo H and Pathak A 2006b Electronic cross sections for proton transport in liquid water based on optical-data models *Nucl. Instrum. Methods B* **249** 26–8

Emfietzoglou D, Nikjoo H and Pathak A 2006c A comparative study of dielectric response function models for liquid water *Radiat. Prot. Dosim.* **122** 61–5

Emfietzoglou D, Nikjoo H, Petsalakis I D and Pathak A 2007b A consistent dielectric response model for water ice over the whole energy-momentum plane *Nucl. Instrum. Methods B* **256** 141–7

Emfietzoglou D, Pathak A and Nikjoo H 2007a Electronic stopping power of liquid water for protons down to the Bragg peak *Radiat. Prot. Dosim.* **126** 97–100

Emfietzoglou D, Pathak A, Papamichael G, Kostarelos K, Dhamodaran S, Sathish N and Moscovitch M 2006a A study on the electronic stopping of protons in soft biological matter *Nucl. Instrum. Methods B* **242** 55–60

Fano U 1963 Penetration of protons, alpha particles, and mesons *Annu. Rev. Nucl. Sci.* **13** 1–66

Fernandez-Varea J M, Mayol R, Liljequist D and Salvat F 1993 Inelastic scattering of electrons in solids from a generalized oscillator strength model using optical and photoelectric data *J. Phys.: Condens. Matter* **5** 3593–610

Fernandez-Varea J M, Mayol R, Salvat F and Liljequist D 1992 A comparison of inelastic electron scattering models based on δ-function representations of the Bethe surface *J. Phys.: Condens. Matter* **4** 2879–90

Ferrell T L and Ritchie R H 1977 Energy losses by slow ions and atoms to electronic excitations in solids *Phys. Rev. B* **16** 115–23

Friedland W, Jacob P, Bernhardt P, Paretzke H G and Dingfelder M 2003 Simulation of DNA damage after proton irradiation *Radiat. Res.* **159** 401–10

Garcia-Molina R, Abril I, Denton C D and Heredia-Avalos S 2006 Allotropic effects on the energy loss of swift H^+ and He^+ ion beams through thin foils *Nucl. Instrum. Methods B* **249** 6–12

Garcia-Molina R, Abril I, Denton C D, Heredia-Avalos S, Kyriakou I and Emfietzoglou D 2009 Calculated depth-dose distributions for H^+ and He^+ beams in liquid water *Nucl. Instrum. Methods B* at press

Grande P L and Schiwietz G 2005 CasP: convolution approximation for swift particles (version 3.1) http://www.hmi.de/people/schiwietz/casp.html

Hayashi H, Watanabe N, Udagawa Y and Kao C C 2000 The complete optical spectrum of liquid water measured by inelastic x-ray scattering *Proc. Natl Acad. Sci.* **97** 6264–6

Heller J M, Hamm R N, Birkhoff R D and Painter L R 1974 Collective oscillation in liquid water *J. Chem. Phys.* **60** 3483–6

Heredia-Avalos S and Garcia-Molina R 2002 Projectile polarization effects in the energy loss of swift ions in solids *Nucl. Instrum. Methods* B **193** 15–9

Heredia-Avalos S, Garcia-Molina R, Fernandez-Varea J M and Abril I 2005 Calculated energy loss of swift He, Li, B, and N ions in SiO_2, Al_2O_3, and ZrO_2 *Phys. Rev.* A **72** 052902

Ichimaru S 1982 Strongly coupled plasmas: high-density classical plasmas and degenerate electron liquids *Rev. Mod. Phys.* **54** 1017–59

ICRU 1984 Stopping Powers for Electrons and Positrons *ICRU Report 37* (Bethesda, MD: ICRU)

ICRU 1993 Stopping Powers and Ranges for Protons and Alpha Particles *ICRU Report 49* (Bethesda, MD: ICRU)

ICRU 2005 Stopping of Ions Heavier Than Helium *ICRU Report 73* (Bethesda, MD: ICRU)

Inokuti M 1971 Inelastic collisions of fast charged particles with atoms and molecules—the Bethe theory revisited *Rev. Mod. Phys.* **43** 297–347

Inokuti M 1996 Remarks on stopping power: its connections with particle transport and with the electronic structure of matter *Int. J. Quant. Chem.* **57** 173–82

Inokuti M, Dehmer J L, Baer T and Hanson J D 1981 Oscillator-strength moments, stopping powers, and total inelastic-scattering cross sections of all atoms through strontium *Phys. Rev.* A **23** 95–108

Inokuti M, Itikawa Y and Turner J E 1978 Addenda: inelastic collisions of fast charged particles with atoms and molecules—the Bethe theory revisited *Rev. Mod. Phys.* **50** 23–35

Jackson J D and McCarthy R L 1972 Z^3 corrections to energy loss and range *Phys. Rev.* B **6** 4131–41

Kamakura S, Sakamoto N, Ogawa H, Tsuchida H and Inokuti M 2006 Mean excitation energies for the stopping power of atoms and molecules evaluated from oscillator-strength spectra *J. Appl. Phys.* **100** 064905

Kramer M, Jakel O, Haberer T, Kraft G, Schardt D and Weber U 2000 Treatment planning for heavy-ion radiotherapy: physical beam model and dose optimization *Phys. Med. Biol.* **45** 3299–317

Kuhr J-C and Fitting H-J 1999 Monte Carlo simulation of electron emission from solids *J. Electron Spectr. Relat. Phenom.* **105** 257–73

Kumazaki Y, Akagi T, Yanou T, Suga D, Hishikawa Y and Teshima T 2007 Determination of the mean excitation energy of water from proton beam ranges *Radiat. Meas.* **42** 1683–91

LaVerne J A and Mozumder A 1986 Effect of phase on the stopping and range distribution of low-energy electrons in water *J. Phys. Chem.* **90** 3242–7

Lindhard J 1976 The Barkas effect—or Z_1^3, Z_1^4-corrections to stopping of swift charged particles *Nucl. Instrum. Methods* **132** 1–5

Luo S, Zhang X and Joy D C 1991 Experimental determination of electron stopping power at low energies *Radiat. Eff. Defects Solids* **117** 235–242

Mermin N D 1970 Lindhard dielectric function in the relaxation-time approximation *Phys. Rev.* B **1** 2362–3

Montanari C C and Miraglia J E 2006 Stopping power of swift dressed ions *Phys. Rev.* A **73** 024901

Nikjoo H, Uehara S, Emfietzoglou D and Brahme A 2008 Heavy charged particles in radiation biology and biophysics *New J. Phys.* **10** 075006

Oddershede J, Sabin J R and Cabrera-Trujillo R 2005 Comparison of shell corrections in the Bohr and Bethe formulations of stopping power *Nucl. Instrum. Methods* B **241** 144–9

Overhauser A W 1971 Simplified theory of electron correlations in metals *Phys. Rev.* B **3** 1888–98

Paganetti H, Niemierko A, Ancukiewicz M, Gerweck L E, Goitein M, Loeffler J S and Suit H D 2002 Relative biological effectiveness (RBE) values for proton beam therapy *Int. J. Radiat. Oncol. Biol. Phys.* **53** 407–21

Paul H 2007a The mean ionization potential of water, and its connection to the range of energetic carbon ions in water *Nucl. Instrum. Methods* B **255** 435–7

Paul H 2007b New developments in stopping power for fast ions *Nucl. Instrum. Methods* B **261** 1176–9

Paul H, Geithner O and Jakel O 2007a The ratio of stopping powers of water and air for dosimetry applications in tumor therapy *Nucl. Instrum. Methods* B **256** 561–4

Paul H, Geithner O and Jakel O 2007b The influence of stopping powers upon dosimetry for radiation therapy with energetic ions *Adv. Quant. Chem.* **52** 289–306

Penn D R 1976 Electron mean free paths for free-electron-like materials *Phys. Rev.* B **13** 5248–54

Penn D R 1987 Electron mean-free-path calculations using a model dielectric function *Phys. Rev.* B **35** 482–486

Pitarke J M and Campillo I 2000 Band structure effects on the interaction of charges particles with solids *Nucl. Instrum. Methods* B **164–165** 147–60

Planes D J, Garcia-Molina R, Abril I and Arista N R 1996 Wavenumber dependence of the energy loss function of graphite and aluminum *J. Electron Spectr. Relat. Phenom.* **82** 23–9

Porter L E and Lin H 1990 Methods of calculating the Barkas-effect correction to Bethe–Bloch stopping power *J. Appl. Phys.* **67** 6613–20

Ritchie R H 1982 Energy losses by swift charged particles in the bulk and at the surface of condensed matter *Nucl. Instrum. Methods* **198** 81–91

Ritchie R H and Howie A 1977 Electron excitation and the optical potential in electron microscopy *Philos. Mag.* **36** 463–81

Ritchie R H, Hamm R N, Turner J E and Wright H A 1978 The interaction of swift electrons with liquid water *6th Symp. on Microdosimetry* (Luxemburg: Harwood Academic) pp 345–54

Ritchie R H, Hamm R N, Turner J E, Wright H A and Bolch W E 1991 Radiation interactions and energy transport in the condensed phase *Physical and Chemical Mechanisms in Molecular Radiation Biology* (New York: Plenum) pp 99–136

Sabin J R and Oddershede J 2005 Stopping power—what next? *Adv. Quantum Chem.* **49** 299–319

Schinner A, Bachlechner M E and Bohm H M 1994 Plasmon damping and proton stopping in jellium *Nucl. Instrum. Methods* B **93** 181–5

Segui S, Dingfelder M, Fernandez-Varea J M and Salvat F 2002 The structure of the Bethe ridge. Relativistic Born and impulse approximation *J. Phys. B: At. Mol. Opt. Phys.* **35** 33–53

Sigmund P 1994 Light-ion stopping near the maximum *Nucl. Instrum. Methods* B **85** 541–50

Sigmund P 1998 Stopping power in perspective *Nucl. Instrum. Methods* B **135** 1–15

Sigmund P 2004 *Stopping of Heavy Ions* (Berlin: Springer)

Sigmund P and Schinner A 2006 Shell correction in stopping theory *Nucl. Instrum. Methods* B **243** 457–60

Sisterson J 2005 Ion beam therapy in 2004 *Nucl. Instrum. Methods* B **241** 713–6

Smith A R 2006 Proton therapy *Phys. Med. Biol.* **51** R491–504

Smith D Y, Inokuti M, Karstens W and Shiles E 2006 Mean excitation energy for the stopping power of light elements *Nucl. Instrum. Methods* B **250** 1–5

Sturm K 1982 Electron energy loss in simple metals and semiconductors *Adv. Phys.* **31** 1–64

Sturm K and Gusarov A 2000 Dynamical correlations in the electron gas *Phys. Rev.* B **62** 474–91

Tan Z, Xia Y, Zhao M and Liu X 2006 Proton stopping power in a group of bioorganic compounds over the energy range of 0.05–10 MeV *Nucl. Instrum. Methods* B **248** 1–6

Tan Z, Xia Y, Zhao M and Liu X 2008 Electronic stopping power for proton in amino acids and protein in 0.05–10 MeV range *Nucl. Instrum. Methods* B **266** 1938–42

Tan Z, Xia Y, Zhao M, Liu X, Li F, Huang B and Ji Y 2004 Electron stopping power and mean free path in organic compounds over the energy range of 20–10,000 eV *Nucl. Instrum. Methods* B **222** 27–43

Tanuma S, Powell C J and Penn D R 2003 Calculation of electron inelastic mean free paths (IMFPs): VII. Reliability of the TPP-2M IMFP predictive equation *Surf. Interf. Anal.* **35** 268–75

Tanuma S, Powell C J and Penn D R 2008 Calculations of stopping powers of 100 eV–30 keV electrons in 31 elemental solids *J. Appl. Phys.* **103** 063707

Uehara S, Toburen L H and Nikjoo H 2001 Development of a Monte Carlo track structure code for low-energy protons in water *Int. J. Radiat. Biol.* **77** 139–54

Uehara S, Toburen L H, Wilson W E, Goodhead D T and Nikjoo H 2000 Calculations of electronic stopping cross sections for low-energy protons in water *Radiat. Phys. Chem.* **59** 1–11

Wang Y-N and Ma T-C 1990 Stopping power and energy-loss straggling of slow protons in a strongly coupled degenerate electron gas *Nucl. Instrum. Methods* B **51** 216–8

Watanabe N, Hayashi H and Udagawa Y 1997 Bethe surface of liquid water determined by inelastic x-ray scattering spectroscopy and electron correlation effects *Bull. Chem. Soc. Japan.* **70** 719–26

Watanabe N, Hayashi H and Udagawa Y 2000 Inelastic x-ray scattering study on molecular liquids *J. Phys. Chem.* **61** 407–9

Wenzel W A and Whaling W 1952 The stopping cross section of D_2O ice *Phys. Rev.* **87** 499–503

Wilson C D, Dukes C A and Baragiola R A 2001 Search for the plasmon in condensed water *Phys. Rev.* B **63** 121101

Winter B, Weber R, Widdra W, Dittmar M, Faubel M and Hertel I V 2004 Full valence band photoemission from liquid water using EUV synchrotron radiation *J. Phys. Chem.* **108** 2625–32

Xu Y J, Khandelwal G S and Wilson J W 1985 Proton stopping cross sections of liquid water *Phys. Rev.* A **32** 629–32

Ziegler J F 1999 Stopping of energetic light ions in elemental matter *J. Appl. Phys.* **85** 1249–72